Islet Neogenesis–Associated Protein (INGAP)-Positive Cell Mass, β-Cell Mass, and Insulin Secretion

Their Relationship During the Fetal and Neonatal Periods

Viviana Madrid, MD, María I. Borelli, MD, Bárbara Maiztegui, MD, Luis E. Flores, MD, Juan J. Gagliardino, MD, and Héctor Del Zotto, MD

Objectives: To study the chronological appearance of pancreatic islet neogenesis–associated protein (INGAP)-positive cells and its correlation with the increase in β-cell mass and function in fetal and neonatal rats.
Methods: Normal Wistar rat embryos (E) at gestational days 15, 17, and 19 (E15, E17, E19) and 7-day-old postnatal rats (P7) were humanely killed to determine body and pancreas weight; blood glucose; glucose and arginine-induced insulin secretion; real-time polymerase chain reaction of Pdx1 and Ngn3; quantitative immunomorphometric analysis of β-cell replication and apoptosis rate, cytokeratin and INGAP cell mass, and Pdx-1– and Ngn3-positive cells.
Results: Body and pancreas weight increased with age (P7 > E19 > E17 > E15; $P < 0.05$). Neonates had higher blood glucose concentrations than embryos ($P < 0.05$). We recorded a simultaneous and significant age-dependent trend of increase in the number of β- and Pdx-1-positive cells, β- and cytokeratin-positive cell mass and β-cell capacity to release insulin in response to glucose and arginine, and decreased β-cell apoptotic rate. These changes closely paralleled the increase in INGAP-positive cell mass.
Conclusions: These findings suggest that INGAP exerts a positive modulatory effect on β-cell mass and its secretory function in fetal and neonatal rats, thus becoming a new component in the multifactorial regulation of such processes.

Key Words: islet neogenesis-associated protein, ontogenesis, β-cell mass, β-cell function, β-cell apoptosis

(*Pancreas* 2012;00: 00–00)

Pancreatic β-cell mass depends on several processes, including the mitotic division of preexisting β cells (replication), their differentiation from stem cells (neogenesis),[1–3] and their apoptosis, all of which are controlled by different hormones, genes, metabolic substrates, and growth factors.[4] Islet neogenesis-associated protein (INGAP) participates in such control in adult hamsters,[5,6] rats,[7] and mice[8,9] through the combination of 2 opposed mechanisms: (*a*) the activation of its expression by specific transcription factors (Pdx-1, NeuroD, Ngn3, and Isl-1) that also modulate pancreas cell differentiation,[10,11] and (*b*) the inactivation of such expression by other transcription factors involved in the final step of cell differentiation. These data, together with the identification of INGAP-positive cells in mouse pancreatic tissue at 15.5 days of gestation,[9] suggest that INGAP would actively participate in the regulation of endocrine cell mass growth and development during pancreatic ontogeny.

Pancreas organogenesis comprises a coordinated and complex interplay of signals and transcriptional networks that lead to a stepwise process of organ development. It starts with the appearance of the dorsal bud of the foregut at embryonic day (E) 9.5 (E9.5) in mice, followed by the ventral bud at E10. By E13.5, the gut rotates, there is a fusion of the buds, and the pancreatic epithelium branches into the surrounding mesenchyme (branching morphogenesis). On E15.5, the secondary transition starts, including fate specification of all differentiated cell types of the adult organ and delamination of the endocrine precursors from the developing epithelium. Finally, during isletogenesis (E17.5), the simultaneous aggregation of endocrine cells into the islets of Langerhans and the development of the exocrine acinar ultrastructure occur. In the early postnatal period, a high percentage of endocrine cells is overtaken by massive growth of the exocrine mass, which becomes condensed to form compact acini. The characteristic glucose-stimulated secretion of insulin starts on postnatal day 7.[12] Because the gestation period for mice is 19 days and that of rats lasts 21 days, it is accepted that the appearance of the aforementioned steps occurs almost 2 days later in rats than in mice.[12]

Based on this knowledge, and to compare the chronological appearance of pancreatic INGAP-positive cells and β cells as well as their mass progression, we currently studied such relationship in normal rat fetuses at E15 (branching morphogenesis of the pancreas), E17 (secondary transition), E19 (isletogenesis), and in 7-day-old postnatal rats (P7).

MATERIALS AND METHODS

Animals

Rats were maintained under controlled conditions of room temperature (21°C ± 1°C) and humidity (50% ± 5%), with a 12-hour light–12-hour darkness cycle and free access to a commercial diet and tap water. The presence of a vaginal plug was considered to be day 0 of pregnancy. After death, fetuses from normal Wistar rats at E15, E17, and E19, as well as 7-day-old neonates (P7) were removed and dissected using a Carl Zeiss stereomicroscope.

Animal experiments and handling were performed according to the *Ethical Principles and Guidelines for Experimental Animals* of the Swiss Academy of Medical Sciences, third edition (2005).

Measurement of Clinical Parameters

Blood glucose of samples obtained from the neck and the umbilical cord of neonates and fetuses, respectively, was measured

From the CENEXA, Centro de Endocrinología Experimental y Aplicada (UNLP, CONICET LA PLATA; Centro Colaborador OPS/OMS), Facultad de Ciencias Médicas UNLP, La Plata, Argentina.
Received for publication February 9, 2012; accepted June 14, 2012.
Reprints: Juan J. Gagliardino, MD, CENEXA (UNLP, CONICET LA PLATA), Facultad de Ciencias Médicas UNLP, 60 y 120, 1900 La Plata, Argentina (e-mail: cenexa@speedy.com.ar).
This study was supported with funds provided by CONICET.
The authors declare no conflict of interest.
MIB, BM, LEF, JJG and HDZ are members of the Research Career of CONICET. These results are part of VM doctoral thesis.

using test strips (One touch Ultra, Lifescan, Milpitas, Calif). Body weight and pancreas weight of embryos and neonates were also recorded.

Immunohistochemical Studies

The abdominal region of E15 and the whole pancreas of E17, E19, and P7 were removed; and the wet weight of the pancreas was recorded. Pancreases were then fixed in 10% formaldehyde and embedded in paraffin. Serial sections of fixed pancreas (5 μm) were obtained from 3 different levels of the blocks with a rotatory microtome and mounted on silanized slides (3-amino-propyltriethoxy-silane [Sigma Co, St Louis, Mo]).[13] Sections were deparaffinized, incubated for 30 minutes in 3% hydrogen peroxide in methanol to block endogenous peroxidase activity, rehydrated in a descending ethanol series, and incubated in 2.5% porcine serum to reduce nonspecific binding. The slides were then incubated for 24 hours at 4°C in a humidified chamber with different appropriately diluted primary antibodies. For the final staining, we used the streptavidin-biotin complex (1:40 and 1:20 respectively; Sigma), peroxidase, or alkaline phosphatase. The incubation period for this step was 30 minutes with the secondary biotinylated antibodies and peroxidase or alkaline phosphatase.

Insulin Immunostaining and Cell Replication Rate

Sequential double staining for proliferating cell nuclear antigen (PCNA; 1:500; Sigma) and β cells (1:20,000; our own guinea pig insulin antibody) was performed. First, PCNA staining was done as described previously using carbazole as chromogen; the same section was then immunostained for β-cell identification as already described, except that alkaline phosphatase and fast blue (Sigma) were used as chromogens. The streptavidin-alkaline phosphatase conjugate was applied to each section for 30 minutes at room temperature; sections were then washed and alkaline phosphatase substrate was applied for another 30 minutes. Sections were further washed and mounted in aqueous medium (Dako North America, Inc, Carpinteria, Calif). Within a given cell type, replication β-cell rate was quantified and expressed as the percentage of PCNA-labeled cells of the total β cells counted. Furthermore, simple controls were done for every immunostaining by omitting the primary antiserum.

Islet Neogenesis (Cytokeratin [CK]-19 Immunostaining)

Deparaffinized sections were pretreated with 250-mL antigen retrieval solution (Vector Laboratories, Burlingame, Calif) for 10 minutes in a 500-W microwave oven.[14] Cytokeratin-positive cells were then revealed using a specific anti-CK19 antibody (Sigma clone 4·62).

β-cell Apoptotic Rate

Apoptotic bodies were identified using the propidium iodide technique.[15] For this purpose, deparaffinized and rehydrated sections were washed in phosphate-buffered saline before incubation for 30 minutes in a dark humidified chamber with a solution of propidium iodide (4 μg/mL; Sigma) and ribonuclease A (100 μg/mL; Sigma). A Zeiss Axiolab epifluorescence microscope equipped with an HBO50 mercury lamp together with 2 different filters was used to identify the auto-fluorescent labeling of apoptotic bodies. Insulin immunofluorescence staining (fluorescein isothiocyanate; FITC) was used to reveal β cells.

For quantitative evaluation, positively labeled apoptotic endocrine cells were counted under a ×40 objective lens in sections obtained from different levels of the blocks. The number of apoptotic cells was expressed as the percentage of the total number of β cells counted.

Detection of Pancreatic Duodenal Homeobox-1 (Pdx-1) and INGAP-Positive Cells

Pancreas sections were sequentially stained with INGAP and Pdx-1 antibodies to identify INGAP- and Pdx-1–positive cells as well as cells coexpressing them. Pdx-1-positive cells were first stained with the Pdx-1 antibody (1:1,000; kindly provided by Dr C Wright, Department of Cell Biology, Vanderbilt University, Nashville, Tenn) and revealed as described earlier using carbazole as chromogen; the same section was then immunostained with the INGAP antibody (1:300), except that alkaline phosphatase and fast blue (Sigma) were used as chromogens. Later, the number and area of cells expressing separately or coexpressing these 2 factors were quantified within islet cells.[16]

Ngn3 Immunostaining

Antigen retrieval was performed as described earlier, and the presence of Ngn3-positive cells was thereafter determined using a specific anti-Ngn3 antibody (1:4000) kindly provided by Dr M German, University of California, San Francisco, Calif.

Morphometrical Analysis

The morphometrical analysis was performed by videomicroscopy using a Nikon Eclipse 80i light microscope and a digital DS-U1 camera in combination with OPTIMAS software (Bioscan Incorporated, Edmons, Wash). We measured the following parameters: total pancreas area excluding connective tissue, endocrine pancreas area (insular and extrainsular), exocrine pancreas area, islet size, β-cell size and volume density of insulin-, INGAP- and CK19-positive cells. To estimate the mass of islet and extrainsular β-, INGAP- and CK-positive cells, we multiplied the respective volume densities by the total weight of the pancreas.[17]

Pdx1 and Ngn3 Gene Expression (Real-Time PCR)

Complementary DNA (cDNA) from E17, E19, and P7 pancreases was obtained using TRIzol Reagent (Gibco-BRL, Rockville, Md) following the manufacturer's instructions. The integrity of the isolated RNA was checked by 1% agarose-formaldehyde gel electrophoresis. Possible contamination with protein or phenol was controlled by measuring the 260:280-nm absorbance ratio, whereas DNA contamination was avoided using DNAase I (1 U/μl; Gibco-BRL). Retrotranscription reaction was performed using 200-U/μL Super Script III reverse transcriptase (Gibco-BRL), oligo dT (Invitrogen, Carlsbad, Calif), and 1 μg of total RNA as template. Negative controls were performed by omission of SuperScript III in the reaction mixture. Quantitative polymerase chain reaction (PCR) was performed with a MiniOpticon real-time PCR detector separate MJR (BioRad, Hercules, Calif) using SYBR Green I as a fluorescent dye and 1/40th of the islet cDNA as template. Reactions were performed in a 25-μL quantitative PCR reaction mixture containing 0.36-μmol/L of each primer, 3-mmol/L $MgCl_2$, 0.2-mmol/L dNTPs, and 40 mU/μL platinum Taq DNA polymerase (Invitrogen). The PCR profile was as follows: a first step of 3 minutes at 95°C followed by 40 cycles of 30 seconds at 95°C, 30 seconds at 65°C and 45 seconds at 72°C, with a final extension step of 10 minutes at 72°C followed by a melting curve from 55°C to 90°C. The optimal parameters for the PCR reactions were empirically defined. Each PCR amplification was performed in triplicate. The oligonucleotide primers (Invitrogen) used were as follows: sequence 5′ to 3′, forward primer (A) and reverse primer (B): Pdx1, A,

ggtgccagagttcagtgcta, and B, acttccctgttccagcgttc (amplicon size, 112 bp; NM_022852) and Ngn3, A, tccaagtgtcccaagagacc and B, agtcacctgcttctgcttcg (amplicon size, 129 bp, NM_021700). β-actin was used as a housekeeping gene (primer sequences: A, agagggaaatcgtgcgtgac and B, cgatagtgatgacctgaccgt; amplicon size, 138 bp; NM_031144). The purity and specificity of the amplified PCR products were verified by performing melting curves and were further checked by 2% (wt/vol) agarose gel electrophoresis and ethidium bromide staining. Data were expressed as relative gene expression with respect to control group after normalization to the β-actin housekeeping gene, by using the delta-delta cycle threshold method.

Insulin Secretion in Vitro

Pieces of fetus (E17 and E19) or postnatal pancreases (P7) were dropped into small tubes containing a membrane filter paper at the bottom[16]; these tubes were immersed into wider tubes containing Krebs-Ringer bicarbonate buffer with bovine serum albumin (BSA), 1% trypsin inhibitor (Trasylol), and 2 different glucose concentrations (3.3 and 16.7 mmol/L) or 10-mmol/L arginine (without glucose), and incubated for 60 minutes at 37°C.[18] At the end of the incubation period, the medium was recovered and kept at −20°C to determine insulin concentration by radioimmunoassay.[19] Dry pancreas weight was recorded to express pancreatic insulin secretion per milligram of tissue.

Statistical Analyses

Quantitative data are expressed as mean ± SEM. The statistical significance was determined by analysis of variance followed by Bonferroni test, considering differences significant when $P < 0.05$.

RESULTS

Clinical and Metabolic Parameters

Body weight increased progressively as a function of age (E15, 0.5 ± 0.01 vs E17, 0.85 ± 0.03 vs E19, 1.84 ± 0.04 vs P7, 12.31 ± 0.22 g; n = 15; $P < 0.05$), and pancreas weight followed a similar growth pattern (E15, 0.8 ± 0.01 vs E17, 1.70 ± 0.07 vs E19, 3.68 ± 0.08 vs P7, 24.07 ± 1.05 mg; n = 15; $P < 0.05$). Whereas blood glucose concentration was comparable in E15, E17, and E19 (59.2 ± 3.5, 61.8 ± 3.08 and 56.6 ± 2.4 mg/dL, respectively), it was significantly higher in P7 (88.13 ± 0.9 mg/dL; n = 15; $P < 0.05$).

β-Cell Mass at Different Stages

Islet β-cell mass was not recorded in E15 owing to the small sample size, but thereafter, it increased gradually and significantly with age ($P < 0.05$; Fig. 1). Considering the value measured in E17 as 100%, the increase recorded in E19 and P7 was 400% and 5600%, respectively, accompanied by a gradual increase in islet size that reached a peak value in P7 (E17, 687.2 ± 86.1 and E19, 958.8 ± 234.6 vs P7, 2235.84 ± 351 μm^2; $P < 0.05$). No significant changes were detected, however, in β-cell size (E17, 92.7 ± 13.13; E19, 105.9 ± 16.7; P7, 74.69 ± 3.8 μm^2). Extrainsular β-cell mass showed a similar growth pattern to that recorded in islet β-cell mass (E17, 0.86 ± 0.2 vs E19, 4.1 ± 1.3 vs P7, 56 ± 13 μg; $P < 0.05$).

Islet Neogenesis, Replication, and Apoptosis

The β-cell replication rate was significantly lower in P7 than in the other stages recorded (E17, 11.7 ± 3.5 and E19, 12.2 ± 6.1 vs P7, 1.97 ± 0.41 %; $P < 0.05$; Fig. 1). Cytokeratin 19–positive cell mass increased significantly between E17 and E19 (220%), reaching its greatest value at P7 (2500%; $P < 0.05$; Fig. 2). The percentage of β-cell apoptosis decreased progressively and significantly with age: at E19 and P7, values were 66% and 20%, respectively, of the value recorded in E17 ($P < 0.05$). This trend was just the opposite of the one displayed by β-cell mass (Fig. 2).

Modulators of β-Cell Mass: Pdx1, Ngn3, and INGAP

The number of Ngn3-positive cells decreased significantly from E17 to E19 (E17, 117.6 ± 26.6 vs E19, 38.7 ± 11 cells/mm^2;

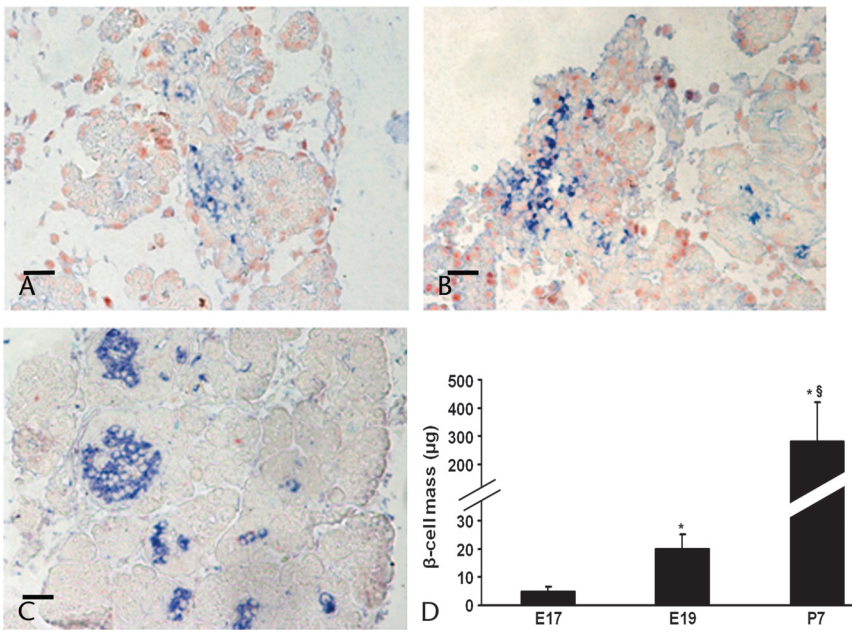

FIGURE 1. Pancreas sections of E17 (A), E19 (B), and P7 (C) immunostained with insulin antibody (blue) and PCNA (nuclei, red). Scale bar = 50 μm × 10, D, Quantitation of insulin-positive β-cell mass. Each bar represents the mean of 3 rat pancreases and sections from 3 different levels of the paraffin block for each age group ± SEM. *Compared to E17; §compared to E19; in all cases, $P < 0.05$.

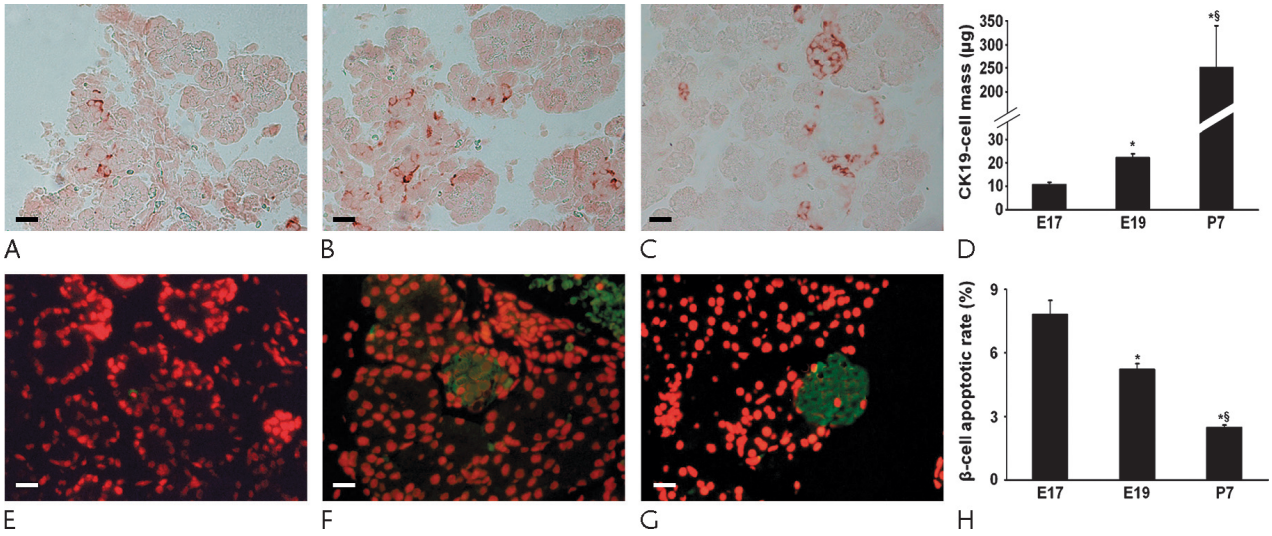

FIGURE 2. Pancreas sections of E17 (A, E), E19 (B, F), and P7 (C, G) immunostained with CK19 antibody (red, A–C) or stained by immunofluorescence with insulin antibody (green, fluorescein isothiocyanate) and propidium iodide (apoptotic nuclei, red; E–G). Scale bar = 50 μm × 10. D, CK19-positive cell mass measured at different ages. H, Percentage of apoptotic β-cells. D, H, Each bar represents the mean ± SEM of 3 pancreases and sections from 3 different levels of the paraffin block for each age group; *compared to E17 and §compared to E19; in all cases, $P < 0.05$.

$P < 0.05$; Fig. 3), being undetectable at P7. The same pattern was followed by Ngn3 mRNA levels ($P < 0.05$; Fig. 3).

The age-dependent β-cell mass increase described earlier was accompanied by a parallel increase in the number of Pdx-1–positive cells (E17, 7.95 ± 3.56 [100%] and E19, 20.9 ± 8.9 [263%] vs P7, 166.1 ± 33.4 [2088%] cells/mm^2; $P < 0.05$; Fig. 4). Pdx1 gene expression increased significantly just 2 days before birth (E19) compared to either E17 or P7 ($P < 0.05$; Fig. 4).

The first scattered INGAP-positive cells appeared in E15 (data no shown), and the INGAP-positive cell mass increased gradually (E17, 100%; E19, 150%; P7, 250%; $P <$

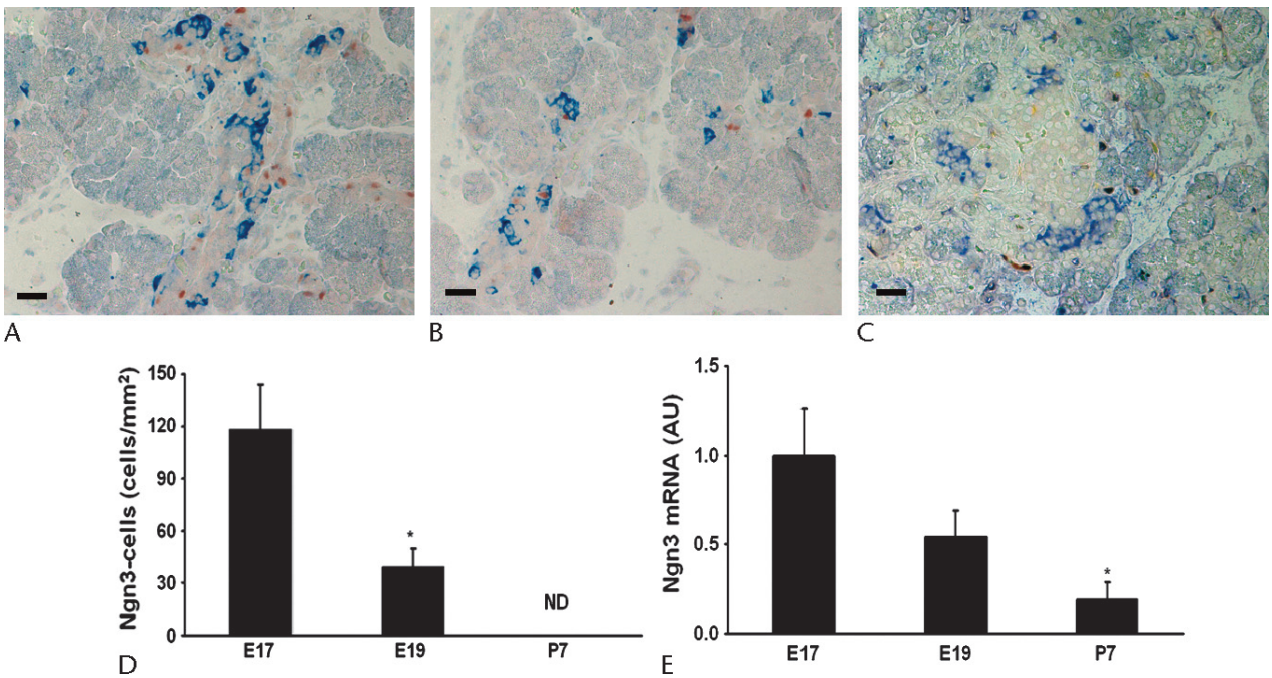

FIGURE 3. Pancreas sections of E17 (A), E19 (B) and P7 (C) immunostained with Ngn-3 (nuclei, red) and non-beta antibody cocktail (blue). Scale bar = 50 μm. ×10. D, Quantitation of the number of Ngn-3 positive cells. Each bar represents the mean ± SEM of 3 pancreases and sections from 3 different levels of the paraffin block for each age group. E, Levels of Ngn-3 mRNA determined by quantitative PCR. Values are expressed in arbitrary units (AU) relative to E17 and represent the mean of 3 independent experiments. D, E, *Compared to E17 and §compared to E19; in all cases, $P < 0.05$.

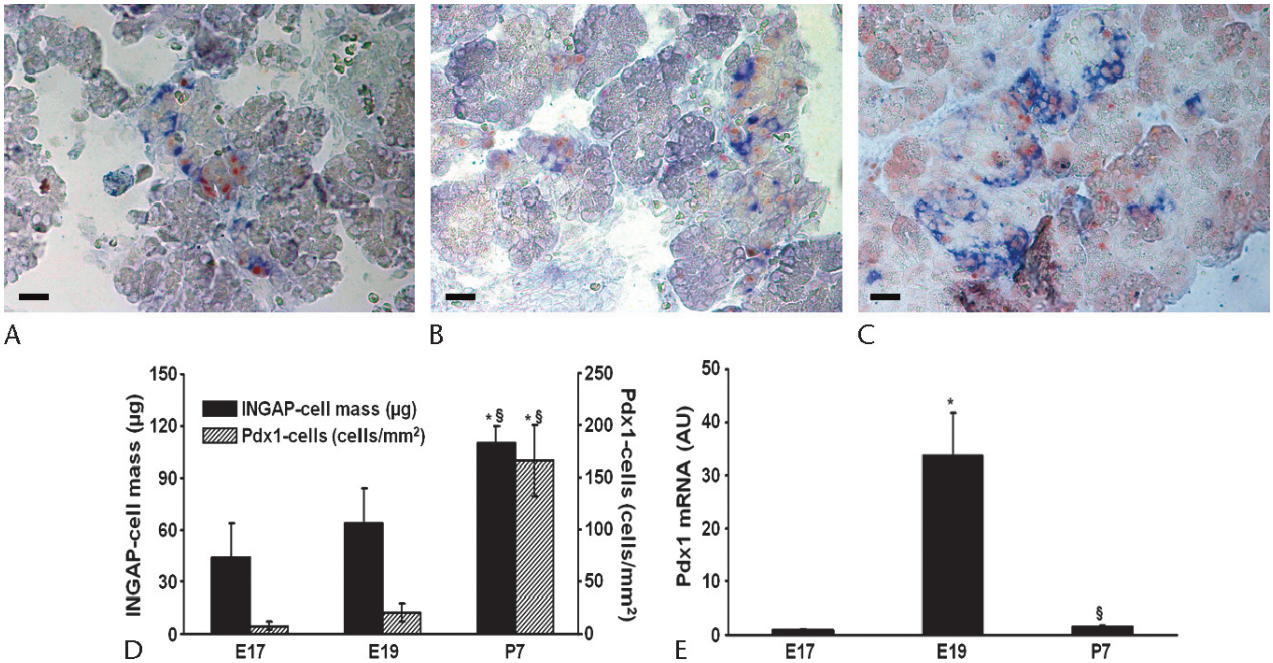

FIGURE 4. Pancreas sections of E17 (A), E19 (B), and P7 (C) immunostained with Pdx-1 (nuclei, red) and INGAP (blue) antibodies. Scale bar = 50 μm × 10. D, Quantitation of INGAP-positive cell mass (black bars, left scale) and number of Pdx-1–positive cells (striped bars, right scale). Each bar represents the mean ± SEM of 3 pancreases and sections from 3 different levels of the paraffin block for each age group. E, Levels of Pdx-1 mRNA determined by quantitative PCR. Values are expressed in AU relative to E17 and represent the mean of 3 independent experiments. D, E, *Compared to E17 and §compared to E19; in all cases, $P < 0.05$.

0.05), reproducing the profile of β-cell mass (Fig. 4). Whereas extraislet INGAP-positive cells were scarce, the largest INGAP-positive cell mass was identified within the islets (Fig. 4).

Insulin Secretion in Vitro

Insulin secretion was not recorded in E15 owing to the scarce amount of available tissue. The E17 and E19 pancreases released in vitro similar amounts of insulin in response to either 3.3- or 16.6-mmol/L glucose, but such release was significantly higher in response to 10-mmol/L arginine ($P < 0.05$; Fig. 5). Conversely, neonatal pancreases secreted more insulin in response to 16.6-mmol/L than to 3.3-mmol/L glucose, and 10-mmol/L arginine as well as 16.6-mmol/L glucose elicited the release of a comparable amount of insulin (Fig. 5). The response to every stimulus but particularly to 16.6-mmol/L glucose rose as a function of age (214% and 940% higher in E19 and P7, respectively, compared to E17; $P < 0.05$).

To better understand the possible relationship of the changes recorded in β-cell mass, CK-positive cells, β-cell apoptosis rate, insulin secretion, and the number of Pdx1- and Ngn3-positive cells with respect to those recorded in the mass of INGAP-positive cells, we plotted the former parameters as a function of the latter (Fig. 6). Whereas a positive relationship

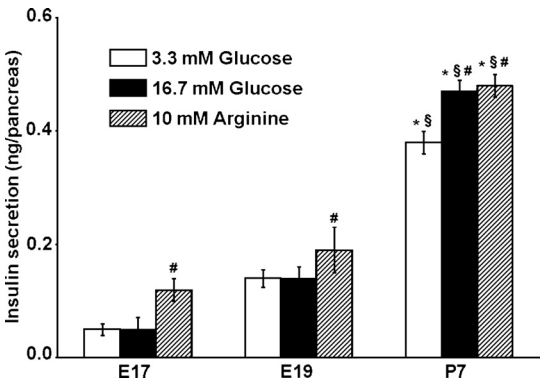

FIGURE 5. Insulin secretion in response to 3.3-mmol/L (white bars) and 16.6-mmol/L (black bars) glucose and 10-mmol/L arginine (striped bars). Each bar represents the mean ± SEM of 6 cases from 3 different experiments. *Compared to E17; §compared to E19; # compared to 3.3-mmol/L glucose; in all cases, $P < 0.05$.

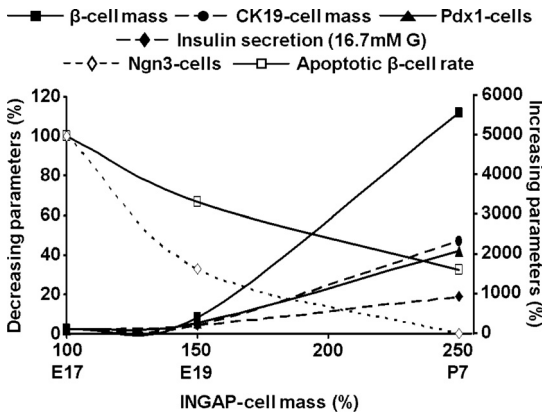

FIGURE 6. Chronological changes in morphological and functional parameters as a function of INGAP-positive cell mass values. In all cases, changes were estimated considering the corresponding E17 value as 100%. Left scale, decreasing parameters: β-cell apoptotic rate and number of Ngn3-positive cells. Right scale, increasing parameters: β- and CK-cell mass, insulin secretion, and number of Pdx-1–positive cells.

was clearly seen among INGAP-positive cell mass, β-cell mass, CK- and Pdx1-positive cells, and insulin secretion, such relationship was negative regarding β-cell apoptosis. Opposite trends were observed in INGAP- and Ngn3-positive cell masses.

DISCUSSION

Our results show that the increase in body and pancreas weight was concomitant with the progression of gestational to postnatal age. However, the ratio body/pancreas weight remained constant at all ages (approximately 0.2%).

Serum glucose levels were significantly lower in E15, E17, and E19 compared with that in P7. These data are consistent with the direct observation of milk in the stomach of P7 at the time of death.

As previously reported by other authors, we found that β-cell mass increased significantly and progressively from E17 to P7.[20,21] This time-dependent upward curve was accompanied by (*a*) a parallel increase in islet size, with no changes in β-cell size, (*b*) an increase in CK-positive cell mass and extrainsular β-cell number, (*c*) an increased number of Pdx-1–positive cells, and (*d*) a significant decrease in apoptotic β-cell rate. Altogether, these data suggest that the increased β-cell mass currently described can be ascribed to an increase in β-cell number consecutive to a combination of increased neogenesis rate and reduced apoptosis rate. This assumption is supported by previous reports on the issue.[20,21] Surprisingly, Pdx-1 mRNA did not show the same pattern because it underwent a peak value at E19, probably preparing cells for the large increase of Pdx-1–positive cells found after birth.

Consistent with already published evidence, we also observed a reverse time-dependent trend in both Ngn-3 gene expression and the number of Ngn3-positive cells: their early and high expression in fetal life decreased as a function of the animal's age.[22,23]

Insulin release in vitro in response to 16.6-mmol/L glucose did not increase in pancreases obtained at gestational days 17 and 19, but it did in response to arginine. By contrast, and as previously reported,[24–27] the secretion of insulin in response to 16.6-mmol/L glucose and arginine increased in neonatal pancreases, being the amount of insulin released significantly higher than that measured in E17 and E19. The lack of recognition of different glucose concentrations by the fetal pancreas has been ascribed to the fact that glucokinase, the key enzyme for its metabolization, is not functionally active at this stage, becoming active in 7-day-old animals.[28] On the other hand, arginine, that is positively charged, is weakly metabolized; but it is transported into the β cell and sequentially triggers a reaction cascade that starts with the plasma membrane depolarization[29] and ends with an increase in the concentration of cytosolic Ca^{+2} that promotes insulin secretion.

We have observed a simultaneous age-dependent trend of increase in the number of β cells, Pdx-1–positive cells, β-cell and CK-positive cell mass, β-cell capacity to release insulin in response to glucose and arginine, together with a decrease in the rate of β-cell apoptosis and the number of Ngn3-positive cells. As clearly depicted in Figure 6, all these changes closely paralleled the increase in the mass of INGAP-positive cells. This parallelism, together with the proven in vivo positive modulatory effect of INGAP upon β-cell mass, its negative effect on β-cell apoptosis,[6] as well as its enhancing effect on insulin secretion either in vitro[27,30] or in vivo,[6] strongly suggests that INGAP exerts a positive modulation on both β-cell mass and its secretory function in fetal and neonatal rats. Furthermore, the opposite pattern exhibited by the mass of Ngn3- and INGAP-positive cells might suggest that whereas the former is the main modulator of β-cell mass in the fetus, INGAP would play such role in the postnatal period. New study approaches are necessary to confirm/discard this assumption.

Despite the consistent evidence currently reported concerning the relationship of β-cell mass/function and INGAP, we must accept, however, that other factors known to affect the β-cell sensitivity threshold to glucose such as glucagon-like peptide 1 and glucose-dependent insulinotropic polypeptide [31–36] as well as growth hormone, prolactin, and placental lactogen[37–39] might also participate in the regulation of those processes.

In brief, our results show a positive relationship of INGAP-positive cell mass with β-cell mass, CK-positive cells and insulin secretion, and a negative one with β-cell apoptosis; these correlations, together with the already known effect of INGAP on β-cell mass and insulin secretion,[6–8,11,16,27,30,40] strongly suggest that INGAP would participate in the regulation of β-cell mass and function not only in adulthood but also during fetal life. This novel information adds a new component to the multifactorial regulation of such process and could help to develop new tools to prevent and treat stages characterized by the decrease and dysfunction of β-cell mass.

ACKNOWLEDGMENTS

The authors thank Adrián Díaz and César Bianchi for skillful technical assistance, and Adriana Di Maggio for careful secretarial support.

REFERENCES

1. Bonner-Weir S. Regulation of pancreatic beta-cell mass in vivo. *Recent Prog Horm Res*. 1994;49:91–104.
2. Bouwens L, Klöppel G. Islet cell neogenesis in the pancreas. *Virchows Arch*. 1996;427:553–560.
3. Leahy JL. Impaired beta-cell function with chronic hyperglycemia: the "overworked beta-cell" hypothesis. *Diabetes Rev.* 1996;4:298–319.
4. Nielsen JH, Serup P. Molecular basis for islet development, growth and regeneration. *Curr Opin Endocrinol Diabetes*. 1998;5:97–107.
5. Rosenberg L, Brown RA, Duguid WP. A new model to the induction of duct epithelial hyperplasia and nesidioblastosis by cellophane wrapping of the hamster pancreas. *J Surg Res*. 1983;35:63–72.
6. Madrid V, Del Zotto H, Maiztegui B, et al. Islet neogenesis-associated protein pentadecapeptide (INGAP-PP): mechanisms involved in its effect upon beta-cell mass and function. *Regul Pept*. 2009;157:25–31.
7. Del Zotto H, Borelli MI, Flores L, et al. Islet neogenesis: an apparent key component of long-term pancreas adaptation to increased insulin demand. *J Endocrinol*. 2004;183:321–330.
8. Rosenberg L, Lipsett M, Yoon JW, et al. A pentadecapeptide fragment of islet neogenesis-associated protein increases beta-cell mass and reverses diabetes in C57BL/6J mice. *Ann Surg*. 2004;240:875–884.
9. Hamblet NS, Shi W, Vinik AI, et al. The Reg family member INGAP is a marker of endocrine patterning in the embryonic pancreas. *Pancreas*. 2008;36:1–9.
10. Taylor-Fishwick DA, Rittman S, Kendall H, et al. Cloning genomic INGAP: a Reg-related family member with distinct transcriptional regulation sites. *Biochim Biophys Acta*. 2003;1638:83–89.
11. Taylor-Fishwick DA, Shi W, Pittenger GL, et al. PDX-1 can repress stimulus-induced activation of the INGAP promoter. *J Endocrinol*. 2006;188:11–621.
12. Pan FC, Wright C. Pancreas organogenesis: from bud to plexus to gland. *Dev Dyn*. 2011;240:530–565.

13. Hsu SM, Raine L, Fanger H. Use of avidin-biotin-peroxidase complex (ABC) in inmunoperoxidase techniques: a comparison between ABC and unlabeled antibody (PAP) procedures. *J Histochem Cytochem*. 1981;29:577–580.
14. Madsen OD, Jensen J, Petersen HV, et al. Transcription factors contributing to the pancreatic beta-cell phenotype. *Horm Metab Res*. 1997;29:265–270.
15. Scaglia L, Cahill CJ, Finegood DT, et al. Apoptosis participates in the remodeling of the endocrine pancreas in the neonatal rat. *Endocrinology*. 1997;138:1736–1741.
16. Gagliardino JJ, Del Zotto H, Massa L, et al. Pancreatic duodenal homeobox-1 and islet neogenesis-associated protein: a possible combined marker of activateable pancreatic cell precursors. *J Endocrinol*. 2003;177:249–259.
17. Bonner-Weir S, Smith FE. Islet cell growth and the growth factors involved. *Trends Endocrinol Metab*. 1994;5:60–64.
18. Gagliardino JJ, Nierle C, Pfeiffer EF. The effect of serotonin on in vitro insulin secretion and biosynthesis in mice. *Diabetologia*. 1974;10:411–414.
19. Herbert V, Lau KS, Gottlieb CW, et al. Coated charcoal immunoassay of insulin. *J Clin Endocrinol Metab*. 1965;25:1375–1384.
20. Bouwens L, Wang RN, De Blay E, et al. Cytokeratins as markers of ductal cell differentiation and islet neogenesis in the neonatal rat pancreas. *Diabetes*. 1994;43:1279–1283.
21. Kaung HL. Growth dynamics of pancreatic islet cell populations during fetal and neonatal development of the rat. *Dev Dyn*. 1994;200:163–175.
22. Jensen J, Heller RS, Funder-Nielsen T, et al. Independent development of pancreatic alpha- and beta-cells from neurogenin3-expressing precursors: a role for the notch pathway in repression of premature differentiation. *Diabetes*. 2000;49:163–176.
23. Schwitzgebel VM, Scheel DW, Conners JR, et al. Expression of neurogenin3 reveals an islet cell precursor population in the pancreas. *Development*. 2000;127:3533–3542.
24. Asplund KS, Westman S, Hellerström C. Glucose stimulation of insulin secretion from the isolated pancreas of foetal and newborn rats. *Diabetologia*. 1969;5:260–262.
25. Asplund KS. The effect of glucose on the insulin secretion in foetal and newborn rats. In: Falkmer S, Hellman B, Taljedal I-B, eds. *The Structure and Metabolism of the Pancreatic Islets*. Oxford, UK: Pergamon Press; 1970:477–484.
26. Edlund H. Developmental biology of the pancreas. *Diabetes*. 2001;50(suppl 1):S5–S9.
27. Borelli MI, Stoppiglia LF, Rezende LF, et al. INGAP-related pentadecapeptide: its modulatory effect upon insulin secretion. *Regul Pept*. 2005;131:97–102.
28. Taniguchi S, Tanigawa K, Miwa I. Immaturity of glucose-induced insulin secretion in fetal rat islets is due to low glucokinase activity. *Horm Metab Res*. 2000;32:97–102.
29. Cherif H, Reusens B, Dahri S, et al. A protein-restricted diet during pregnancy alters in vitro insulin secretion from islets of fetal Wistar rats. *J Nutr*. 2001;131:1555–1559.
30. Barbosa H, Bordin S, Stoppiglia L, et al. Islet neogenesis associated protein (INGAP) modulates gene expression in cultured neonatal rat islets. *Regul Pept*. 2006;136:78–84.
31. Holst JJ. The physiology of glucagon-like peptide 1. *Physiol Rev*. 2007;87:1409–1439.
32. Aaboe K, Krarup T, Madsbad S, et al. GLP-1: physiological effects and potential therapeutic applications. *Diabetes Obes Metab*. 2008;10:994–1003.
33. Holst JJ, Deacon CF, Visbøll T, et al. Glucagon like peptide-1, glucose homeostasis and diabetes. *Trends Mol Med*. 2008;14:161–168.
34. Padidela R, Patterson M, Sharief N, et al. Elevated basal and post-feed glucagon-like peptide 1 (GLP-1) concentrations in the neonatal period. *Eur J Endocrinol*. 2009;160:53–58.
35. Soltani N, Kumar M, Glinka Y, et al. In vivo expression of GLP-1/IgG-Fc fusion protein enhances beta-cell mass and protects against streptozotocin-induced diabetes. *Gene Ther*. 2007; 14:981–988.
36. Buteau J. GLP-1 receptor signaling: effects on pancreatic beta-cell proliferation and survival. *Diabetes Metab*. 2008;34(suppl 2):S73–S77.
37. Brelje TC, Sorenson RL. The physiological roles of prolactin, growth hormone and placental lactogen in the regulation of islet β-cell proliferation. In: Sarvetnick N, eds. *Pancreatic Growth and Regeneration*. Basel, Swizerland: Karger Landes Systems; 1997:1–30.
38. Nielsen JH. Growth and function of the pancreatic beta cell in vitro: effects of glucose, hormones and serum factors on mouse, rat and human pancreatic islets in organ culture. *Acta Endocrinol Suppl (Copenh)*. 1985;266:1–39.
39. Swenne I. Pancreatic beta-cell growth and diabetes mellitus. *Diabetologia*. 1992;35:193–210.
40. Rosenberg L. In vivo cell transformation: neogenesis of beta cells from pancreatic ductal cells. *Cell Transplant*. 1995;4:371–384.